Evaluating Two Respiratory Correction Methods for Abdominal PET/MRI Imaging

Weiwei Ruan
Wuhan Xiehe Hospital: Wuhan Union Hospital
Fang Liu
Wuhan Xiehe Hospital: Wuhan Union Hospital
Xun Sun
Wuhan Xiehe Hospital: Wuhan Union Hospital
Fan Hu
Wuhan Xiehe Hospital: Wuhan Union Hospital
Tingfan Wu
General Electric Company
Yongxue Zhang
Wuhan Xiehe Hospital: Wuhan Union Hospital
Xiaoli Lan (xiaoli_lan@hust.edu.cn)
Union Hospital, Tongji Medical College, Huazhong University of Science & Technology
https://orcid.org/0000-0002-7263-7399

Original research

Keywords: PET/MRI, respiratory motion correction, standard uptake value, abdomen

Posted Date: May 6th, 2021

DOI: https://doi.org/10.21203/rs.3.rs-488911/v1

Version of Record: A version of this preprint was published at EJNMMI Physics on January 31st, 2022.
See the published version at https://doi.org/10.1186/s40658-022-00430-w.

Abstract

Background: To evaluate two respiratory correction methods for abdominal PET/MRI images, further to analyse the effects on standard uptake values (SUVs) of respiratory motion correction. 17 patients with 25 abdominal lesions on ^{18}F-FDG PET/CT were scanned with PET/MRI. PET images were reconstructed using end-expiratory respiratory gating and multi-bin respiratory gating. Meanwhile, full data and the first 3 minutes and 20 seconds of data acquired both without respiratory gating were reconstructed for evaluation. Five parameters, including the SUV_{max} and SUV_{mean} in the lesions, the SUV_{mean} and standard deviation (SD) in the background, and the signal-to-noise ratio (SNR) were calculated, and used for statistical comparisons. The differences in multi-bin respiratory gating and reconstruction of full data, relative to the reconstruction of the first 3 minutes and 20 seconds of data acquired, were calculated.

Results: Compared with PET/CT, the longer scanning time of abdominal PET/MRI makes respiratory motion correction necessary. The multi-bin respiratory gating correction could reduce the PET image blur and increase the SUV_{max} (11.98%) and SUV_{mean} (13.12%) of the lesions significantly (p = 0.00), which was much more effective than end-expiratory respiratory gating for abdominal PET/MRI. There was no significant difference in the increase in SUV_{max} between multi-bin respiratory gating correction and associated count loss with the correction (p=0.39), which was rarely reported by previous studies.

Conclusion: The multi-bin respiratory gating is proposed as the default reconstruction method for abdominal PET/MRI. However, the respiratory gating correction with the PET counts loss would induce the falsely improvement for SUV_{max} of lesions.

Background

Positron emission tomography (PET) uses radiotracers to image functional changes for detecting diseases. It is usually more sensitive and can detect disease foci earlier than structural imaging [1]. PET is critical for the staging and assessment of treatment response in many cancers. The standardised uptake value (SUV) is usually used in PET [2, 3]. Accuracy of uptake measurement is vital.

Respiratory motion during scanning can blur images, affect the SUVs of images, and cause bias in its measurement [4]. Many methods for correcting respiratory motion in PET imaging have been reported [5–7]. The key thinking has been to isolate the quiescent period based on the patient's measured respiratory waveform (amplitude or phase). For example, end-expiration respiratory gating is based on the observation that the patients usually have a quiescent period after end-expiration during the breathing cycle. Only the counts acquired during the quiescent period were considered valid and used for reconstruction [8, 9]. However, these respiratory motion correction methods are seldom used in routine clinical scanning. For PET/CT, whole body scanning usually requires only 2 minutes per bed position, and the speed of scanning has been increasing with the improvement of PET detectors [10], which has limited the effects of respiratory motion.

PET/MRI has been in clinical use for over 10 years [11]. PET/MRI has many advantages over PET/CT, especially improved soft tissue contrast and the elimination of ionizing radiation from CT. The combination of PET and multi-sequence MRI, that is, T1-weighted (T1WI), T2-weighted (T2WI), and diffusion-weighted imaging (DWI), provides more information for diagnosis. However, the characters of multi-sequences scanning for PET/MRI decided the scanning time much longer than that for PET/CT. Even for single-site scanning, the time often approximate 10 minutes. With this increased scanning time, the effects of respiratory motion on PET images will increase, making respiratory motion correction necessary.

The most commonly utilized respiratory motion correction technique is end-expiration respiratory gating. The system in our PET/MRI (Q.Static, GE Healthcare) uses this quiescent part of the respiratory cycle. End-expiratory respiratory gating has two key parameters, offset and width [8], and it relies on the frequency and amplitude of the respiratory cycle (Fig. 1). The offset determines the initial point for the quiescent phase and the width represents the proportion of the quiescent time in the respiratory cycle. Grootjans et al. used a pressure sensor integrated in an elastic belt placed around the patient's thorax and reconstructed the images with 50%, 35%, and 20% of acquired PET data (respiratory cycle) for respiratory motion correction. Their optimal respiratory-gated images were reconstructed with a duty cycle of 35% [12]. Hope et al. evaluated the effects of end-expiratory respiratory gating for liver PET images using six patients' ^{68}Ga-DOTATATE PET/MRI scans. Their results suggest that SUV_{max} improved significantly compared with ungated data, which used the 50% of the respiratory period from accepted breath-holds for the final reconstruction [13]. Another respiratory motion correction technique is multi-bin respiratory gating (Fig. 1), which is used to replay gated images to eliminate respiratory motion by subdividing the data into bins (phases) to better visualize the respiratory cycle. The method does not depend on the amplitude of the respiratory cycle.

The SUV_{max} calculations are sensitive to noise and values improved with less scan times as image noise increases, which has been demonstrated in previous works [14]. For the PET reconstruction with respiratory motion correction, there are two reasons effecting the SUVs. On the one hand, the reducing of respiratory blurring will increase measured SUVs [15]. On the other hand, the respiratory motion correction isolated the PET counts with consistent respiratory amplitude or phase and dropped others, which means the less PET counts and increased the image noise. However, the comparisons of the two reason on effecting the SUVs were rarely reported.

Here, we compared the two respiratory motion correction methods, end-expiratory respiratory gating and multi-bin respiratory gating in abdominal PET/MRI, which was evaluated with measured SUV both in lesions and the background. The aim of this study was to evaluate two respiratory motion correction methods and further explore how to balance respiratory motion and the lost counts due to respiratory motion correction in abdominal PET/MRI.

Methods

Patients

This was a retrospective study. ^{18}F-FDG PET/MRI was performed in patients with lesions with obvious high uptake in the abdomen on ^{18}F-FDG PET/CT images. After the scanning of the PET/CT, the patients performed the PET/MRI scanning without extra injection of ^{18}F-FDG. The exclusion criteria were any contraindication against MRI scanning [16]. Patients demonstrating obvious body movement during the PET/MRI scanning were also excluded. Finally, 17 patients with 25 obvious abdominal lesions were included. The study was approved by the Ethics Committee of Tongji Medical College, Huazhong University of Science and Technology. The need for written informed consent was waived.

Imaging Protocol

Patients underwent ^{18}F-FDG PET/MRI imaging of the abdomen in a PET/MRI scanner (3.0 T, SIGNA TOF-PET/MRI, GE Healthcare). Before scanning, respiratory bellows were fastened to the abdomen for respiratory monitoring.

PET acquisition was conducted in Respiratory Gating Mode and all PET data were acquired and stored by list-mode data. The scanning time was 10 minutes. During the PET acquisition, four common abdominal MRI sequences were acquired: (1) MRI-based attention correction (MRAC) sequence based on Dixon water–fat separation; (2) axial T_2WI with fat suppression, which were free-breathing because of the breathing trigger; (3) axial DWI with fat suppression, which were free-breathing due to the breathing trigger; and (4) three-dimensional liver acceleration volume acquisition (LAVA) T_1WI, during which the patient was asked to hold their breath for 18 s during scanning.

PET reconstruction

PET images were reconstructed in four ways (Fig. 1). The first method used full data for reconstruction without respiratory gating (Fig. 1A). The end-expiratory respiratory gating mode used only the data acquired at end-expiration, in which the offset and width were both set at 33% based on the breathing amplitude, which were close to the 35% suggested by previous reports [12] (Fig. 1B). The multi-bin respiratory gating mode processed data that were divided into three phases for every respiratory cycle (Fig. 1C). The processing time used for reconstruction was consistent with the end-expiratory respiratory gating mode, which was nearly 3 minutes 20 seconds (Fig. 1D). To avoid the influence of time, for the fourth way, the data of the first 3 minutes 20 seconds without respiratory gating was also reconstructed. Except for the difference in respiratory motion correction, the other construction parameters were all the same: the ordered subsets expectation maximum (OSEM) algorithm with TOF technique was used for construction, FOV = 60 cm × 60 cm, Matrix = 192 × 192, Filter Cut-off = 3.0 mm, Subsets = 28, Iterations = 2. The attenuation correction of PET was based on MRI data and combined tissue segmentation and template matching methods [17].

Qualitative evaluation of SUV

Quantitative calculations were used to evaluate PET image quality, the following five parameters: the SUV_{max} and SUV_{mean} of lesions, the SUV_{mean} and standard deviation (SD) of the background, and the signal-to-noise ratio (SNR) for each lesion. The SNR was calculated as follows [6]:

$$SNR = SUVL/SD, \quad (1)$$

where "SUVL" represents the SUV_{mean} of lesions and SD represents the standard deviation of the background. SNR is a common parameter used to evaluate the quality of PET images. The SUV_{max} of the background was not used here, concerning about the vulnerability of single-pixel measurements to unstable electronic and environmental noise [18].

Further, we calculated the differences among all parameters (except SUV_{mean} of the background), that is, reconstruction of full data without respiratory gating and multi-bin respiratory gating groups relative to reconstruction of the first 3 minutes and 20 seconds of data acquired without respiratory gating.

The 3D volume of lesions was calculated using 42% threshold segmentation. The region of interest of the background was used with a 3-mm-diameter spheroidal. All work was completed in GE AW workstation 4.6 (GE Healthcare).

Statistical analysis

First, we aimed to compare the differences among the five quantitative parameters in the four groups to evaluate for significance. The homogeneity of the variance distribution of the data for every parameter was tested with the Levene statistic. After verifying the variance distribution to be homogeneous, the following statistical analysis was completed by two-way analysis of variance of randomized block design.

Second, we aimed to analyse whether the results of differences in reconstruction of all data without respiratory gating and multi-bin respiratory gating groups relative to the reconstruction of the first 3 minutes and 20 seconds of data acquired without respiratory gating group were significantly different. The variance distribution was also tested with the Levene statistic. If the variance was homogeneous, the independent *t*-test was used for the following analysis. Otherwise, the Mann–Whitney *U*-test was used.

For the homogeneity of variance test, a $p > 0.05$ was considered homogeneous. For the mean value testing, $p < 0.05$ was considered a statistically significant difference. Statistics were analysed using SPSS Statistics (version 24; IBM).

Results

Table 1 lists the mean values and SDs for the overall data. The statistical testing for variance homogeneity suggested that variances for every parameter in the four groups were all homogeneous ($p > 0.05$). Therefore, it was reasonable to use two-way analysis of variance of randomized blocks for the

statistical comparisons to test the paired data in the four groups and obtain statistical results. The different percentages between pairs of groups were also calculated and are shown in Table 1.

Table 1
Mean and standard deviation (SD) for the five parameters in all four groups are listed. For obvious comparisons, the per cent difference between pairs of groups was also calculated and shown.

		SUV_{max} (Lesions)	SUV_{mean} (Lesions)	SUV_{mean} (Background)	STD (Background)	SNR
Mean ± STD	**[1]Method 1**	8.34 ± 3.02	4.81 ± 1.96	1.69 ± 0.35	0.28 ± 0.18	22.81 ± 15.28
	[2]Method 2	8.32 ± 3.23	4.98 ± 2.07	1.68 ± 0.34	0.37 ± 0.21	16.94 ± 11.07
	[3]Method 3	9.83 ± 3.67	5.73 ± 2.36	1.69 ± 0.33	0.37 ± 0.22	19.36 ± 12.03
	[4]Method 4	8.84 ± 3.30	5.11 ± 2.15	1.70 ± 0.34	0.35 ± 0.20	18.47 ± 13.43
Variance Testing	**F-value (p-value)**	0.96 (0.42)	0.87 (0.46)	0.02 (0.99)	1.06 (0.37)	0.91 (0.44)
Difference Percent (p-value)	**2 vs 1**	2.90% (0.22)	3.09% (0.25)	-0.53% (0.41)	36.68% **(0.00)**	-23.52% **(0.00)**
	3 vs 1	18.15% **(0.00)**	19.70% **(0.00)**	0.46%(0.76)	36.98% **(0.00)**	-11.30% **(0.00)**
	4 vs 1	5.76% **(0.03)**	5.99% **(0.04)**	0.63%(0.55)	31.41% **(0.00)**	-18.00% **(0.00)**
	2 vs 4	-2.28% (0.37)	-2.35% (0.35)	-1.01%(0.16)	4.53% **(0.03)**	-5.93% (0.08)
	3 vs 4	11.98% **(0.00)**	13.12% **(0.00)**	-0.10%(0.78)	5.05% **(0.03)**	9.39% (0.30)
	3 vs 2	15.41% **(0.00)**	17.54% **(0.00)**	1.04% (0.26)	0.64%(0.96)	19.18% **(0.01)**

1 the reconstruction of full data without respiratory gating

2 the reconstruction of end-expiratory respiratory gating

3 the reconstruction of multi-bins respiratory gating

4 the reconstruction of first 3 minutes and 2 seconds data without respiratory gating

For the SUV_{max} and SUV_{mean} of lesions, the values in the multi-bin respiratory gating group were largest. The SUV_{max} and SUV_{mean} increased 11.98% and 13.12%, respectively, compared with the reconstruction of the first 3 minutes and 20 seconds of data acquired without respiratory gating group ($p = 0.00$). These values in the end-expiratory respiratory gating group showed no significant difference with those in the reconstruction of the first 3 minutes and 20 seconds of data acquired the group without respiratory gating ($p = 0.37$). The values for the SUV_{max} and SUV_{mean} of lesions were lowest in the group with reconstruction of full data without respiratory gating.

For the SUV_{mean} of the background, there were no significant differences among all four groups. For the SD of the background, the values in the reconstruction of full data without respiratory gating were the lowest, which means the noise level was lowest if the PET was reconstructed in this way. The SDs in the multi-bin respiratory gating and end-expiratory respiratory gating groups were both slightly larger than those in the reconstruction of the first 3 minutes and 20 seconds of data acquired without respiratory gating group (4.53% and 5.05%, respectively), which means the methods with respiratory gating both increased background noise. Although the SNR in the group with reconstruction of full data without respiratory gating was the highest, the value in the multi-bin respiratory gating group also improved by 19.18%, which was significant ($p = 0.01$) compared with that in the end-expiratory respiratory gating group. The paired comparisons of the datasets are shown in Fig. 2. The results are consistent with those shown in Table 1.

Differences shown in Table 2 were calculated by subtracting the values between the reconstruction of full data without respiratory gating and reconstruction of the first 3 minutes and 20 seconds of data acquired without respiratory gating, and between multi-bin respiratory gating and reconstruction of the first 3 minutes and 20 seconds of data acquired without respiratory gating. Initial variance testing was also conducted for every parameter. The different SUV_{max} and SUV_{mean} values in the lesions showed that variance was not homogeneous ($p = 0.006$ and 0.005,respectively). In subsequent analysis, the Mann–Whitney U-test were used, and the differences in SUV_{max} and SUV_{mean} were not significant ($p = 0.39$). The variances of the other two parameters were homogeneous ($p > 0.05$). The independent *t*-test was used, and the results suggested that the SD and SNR were all significantly different between the two difference calculation groups ($p = 0.00$). The corresponding results are shown in box-plots in Fig. 3, which displays the comparisons of the two groups.

Table 2
Lists of the differences for the reconstruction of full data without respiratory gating and multi-bin respiratory gating relative to the reconstruction of the first 3 minutes and 20 seconds of data acquired without respiratory gating, including the mean value, SD and the corresponding statistical results.

		Lesions		Background	
		SUV_{max}	SUV_{mean}	STD	SNR
Difference (Mean ± STD)	**A**	0.5 ± 0.58	0.30 ± 0.35	-0.07 ± 0.04	4.34 ± 3.99
	B	0.99 ± 1.44	0.61 ± 0.88	0.02 ± 0.04	0.89 ± 3.82
Variance Testing	**F-value (p-value)**	8.25 (0.006)	8.54(0.005)	0.52(0.475)	0.66(0.42)
Mean Value Testing	**p-value**	Z=-0.85 $p = 0.39$	Z=-0.84 $p = 0.40$	0.00	0.00

*A and B represented the differences of the reconstruction of full data without respiratory gating and multi-bins respiratory gating relative to the reconstruction of first 3 minutes and 20 seconds of data, respectively.

Figure 4 displays four representative abdomen PET images shown by 3D maximum intensity projection (MIP). The images showed that the lesion was more intense and sharply defined in the image reconstructed by multi-bin respiratory gating than in the other three images, consistent with the statistical results. The background noise in the images reconstructed by reconstruction of full data without respiratory gating was much lower than that in other reconstructed images, which was consistent with the statistical results.

Discussion

In this study, we evaluated the effects of two respiratory motion correction methods for abdominal PET images obtained by PET/MRI, in which the respiratory correction is considered more important than that in PET/CT. Compared with the reconstruction of the first 3 minutes and 20 seconds of data acquired without respiratory gating, the results suggested that multi-bin respiratory gating correction could reduce the PET image blur induced by respiratory motion and increase the SUV_{max} and SUV_{mean} of the lesions significantly, which was much more effective than end-expiratory respiratory gating for abdominal PET/MRI images. However, respiratory motion correction had little effect on the SUV_{mean} of the background, but did increase the background noise and decreased the SNR of PET images because PET counts were discarded.

Although the SUV_{max} of the lesions was significantly higher in the multi-bin respiratory gating group, which was consistent with previous most reports [6, 19–21], the higher SUV_{max} in multi-bin respiratory

gating can be traced to two reasons, the results of respiratory motion correction and the increase in image noise with the lower PET counts. The comparisons of different of SUV_{max} in the lesions between the reconstruction of full data without respiratory gating and multi-bin respiratory gating, relative to the reconstruction of the first 3 minutes and 20 seconds of data acquired without respiratory gating, did not show significant differences, which suggests that the significant increase of SUV_{max} in lesions after the respiratory motion correction should have relatively high falsely increase induced by the counts reducing. The corresponding analysis was rarely reported by the previous studies. Although the motion artifact of PET images has been reduced after the respiratory motion correction, it probably was that the accuracy of SUVs for the lesions did not improved. Therefore, future studies should develop the respiratory motion correction method without discarding any PET counts.

The multi-bin respiratory gating methods divided the PET data into different phases and used the same phase for reconstruction according to the respiratory cycle. The image blur induced by respiratory motion was reduced and the SUV_{max} and SUV_{mean} for the lesions increased significantly. However, the results of end-expiratory respiratory gating were inconsistent with those of many previous reports [8, 9, 22]. According to the model of end-expiratory respiratory gating as shown in Fig. 1, PET data were collected depending on the amplitude of the respiratory cycle. If the respiratory cycle was not stable and the amplitude decreased irregularly, end-expiratory respiratory gating would reject the counts in the duty cycle, which would affect the PET quality. When the respiratory curve is stable, the lesion in the images from end-expiratory respiratory gating was clearer than that from other methods. In the clinic, we found that the respiratory cycle was often unstable in PET/MRI scanning, which may be because of the following reasons: compared with PET/CT, the bore diameter for the PET/MRI is 10 cm narrower. Second, strong audible noise is always present during the scanning. Third, some MRI sequences during the scanning required patients to hold their breath, which would disrupt the rhythm of respiratory.

There were two parameters for the end-expiratory respiratory gating, offset and width. Results of end-expiratory respiratory gating were also likely related to the parameter settings. To keep the useful time consistent with multi-bin respiratory gating, the offset and width were both set at 33%. The 33% width was also used following a previous recommendation by Grootjans et al., who found that a duty cycle of 35% could provide the best balance between image quality and motion rejection and was thought optimal on ^{18}F-FDG PET imaging of lung cancer by PET/CT [12]. However, in a study by Hope et al., the width was also 50%. They found that end-expiratory respiratory-gated liver PET/MRI images increased SUVs and reduced respiratory blurring [23]. Therefore, future studies should further explore the optimal parameters for the end-expiratory respiratory gating for hybrid PET/MRI.

There were some limitations to this study. Although the results of multi-bin respiratory gating were better than those of end-expiratory respiratory gating with the given parameters, the effect on the fusion of the PET and MRI images was not evaluated in the paper. Second, the scanning of PET/MRI scanning was usually after PET/CT delayed imaging, so the beginning time of scanning of PET/MRI after the injection of tracer was inconsistent. Finally, the numbers of patients used for the studies was not enough and the statistical deviation probably influenced the results.

Conclusions

For abdominal PET/MR imaging, the long scanning time make it more necessary for PET respiratory motion correction than PET/CT. In this study, the results of multi-bin respiratory gating were better than the most common method of end-expiratory respiratory gating with the given parameters. Compared with reconstruction without respiratory correction, multi-bin respiratory gating reduced peripheral blurring of lesions in PET images. It also increased the SUVs of lesions, with two reasons, the respiratory correction and the increasing image noise with the correction. The results suggested there was no significant difference in the increase of SUV_{max} between the two reasons, which was less reported by previous studies. Therefore, multi-bin respiratory gating is proposed as the default reconstruction method for abdominal imaging with PET/MRI. However, the respiratory gating correction with the PET counts loss would also induce the falsely improvement for SUV_{max} of lesions.

List Of Abbreviations

SUV Standard uptake values

SD Standard deviation

PET/MRI Positron Emission Tomography/Magnetic Resonance Imaging

MRAC MRI-based attention correction

LAVA Liver acceleration volume acquisition

Declarations

Ethics approval and consent to participate

This study is a retrospective study based on data from our clinical studies on PET/MR, in which all patients signed informed consent forms and the ethical approval was obtained by the Ethics Committee of Tongji Medical College, Huazhong University of Science and Technology

Consent for publication

Not applicable

Availability of data and material

The datasets used and/or analysed during the current study are available from the corresponding author on reasonable request.

Competing interests

The authors declare that they have no competing interests

Funding

This study has received funding by the National Natural Science Foundation of China (No. 81901735 and 81701759), the Key Project of Hubei Province Technical Innovation (2017ACA182), and the Clinical Research Physician Program of Tongji Medical College, Huazhong University of Science and Technology (No. 5001530008).

Authors' contributions

Dr. Xiaoli Lan: substanti al contributions to conception and design, analysis and interpretation of data, and revising the manuscript critically for important intellectual content. Dr. Weiwei Ruan: contributions to conception and design, acquisition of data, analysis and interpretation of data, and drafting the article. Dr. Fang Liu, Dr. Xun Sun, Ms. Fan Hu, and Dr. Yongxue Zhang: analysis and interpretation of data and drafting the article. Dr. Tingfan Wu: analysis of data. The authors read and approved the final manuscript.

Acknowledgements

Not applicable

References

1. Deng XY, Rong J, Wang L, Vasdev N, Zhang L, Josephson L et al. Chemistry for Positron Emission Tomography: Recent Advances in C-11-, F-18-, N-13-, and O-15-Labeling Reactions. Angew Chem-Int Edit. 2019; 58(9):2580-2605.
2. Lin C, Itti E, Haioun C, Petegnief Y, Luciani A, Dupuis J et al. Early 18F-FDG PET for prediction of prognosis in patients with diffuse large B-cell lymphoma: SUV-based assessment versus visual analysis. J Nucl Med. 2017; 48:1626–1632.
3. Weber WA, Petersen V, Schmidt B, Tyndale-Hines L, Link T, Peschel C et al. Positron emission tomography in nonsmall-cell lung cancer: prediction of response to chemotherapy by quantitative assessment of glucose use. J Clin Oncol. 2003; 21:2651–2657.
4. Nehmeh SA, Erdi YE. Respiratory motion in positron emission tomography/computed tomography: a review. Semin Nucl Med. 2008; 38:167–176.
5. Apostolova I, Wiemker R, Paulus T, Kabus S, Dreilich T, van den Hoff Joerg et al. Combined correction of recovery effect and motion blur for SUV quantification of solitary pulmonary nodules in FDG PET/CT. Eur Radiol. 2010; 20(8): 1868-1877.
6. Minamimoto R, Mitsumoto T, Miyata Y, Sunaoka F, Morooka M, Okasaki M et al. Evaluation of a new motion correction algorithm in PET/CT: combining the entire acquired PET data to create a single three-dimensional motion-corrected PET/CT image. Nucl Med Commun. 2016; 37(2): 162-170.

7. van Elmpt W, Hamill J, Jones J, De Ruysscher D, Lambin P,Öllers M. Optimal gating compared to 3D and 4D PET reconstruction for characterization of lung tumours. Eur J Nucl Med Mol Imaging. 2011; 38(5): 843-855.
8. Liu C, Alessio A, Pierce L, Thielemans K, Wollenweber S, Ganin A et al. Quiescent period respiratory gating for PET/CT. Med Phys. 2010; 37: 5037–5043.
9. van der Vos CS, Grootjans W, Meeuwis APW, Slump CH, Oyen WJG, de Geus-Oei LFF et al. Comparison of a free breathing CT and an expiratory breath-hold CT with regard to spatial alignment of amplitude-based respiratory-gated PET and CT images. J Nucl Med Technol. 2014; 42:269–273.
10. Lamprou E, Gonzalez AJ, Sanchez F, Benlloch JM. Exploring TOF capabilities of PET detector blocks based on large monolithic crystals and analog SiPMs. Physica Med. 2020; 70:10–18.
11. Pichler BJ, Kolb A, Nägele T, Schlemmer HP. PET/MRI: paving the way for the next generation of clinical multimodality imaging applications. J Nucl Med. 2010; 51(3):333–336.
12. Grootjans W, de Geus-Oei L-F, Meeuwis AW, van der Vos CS, Gotthardt M, Oyen WJG et al. Amplitude-based optimal respiratory gating in positron emission tomography in patients with primary lung cancer. Eur Radiol. 2014; 24:3242–3250.
13. Walker MD, Morgan AJ, Bradley KM, McGowan, DR. Evaluation of data-driven respiratory gating waveforms for clinical PET imaging. EJNMMI Res.2019. DOI: 10.1186/s13550-018-0470-9
14. Lodge MA, Chaudhry MA, Wahl RL. Noise considerations for PET quantification using maximum and peak standardized uptake value. J Nucl Med. 2012; 53:1041–1047.
15. Liu C, Pierce LA, Alessio AM, Kinahan PE. The impact of respiratory motion on tumor quantification and delineation in static PET/CT imaging. Phys Med Biol. 2009; 54:7345–7362.
16. Baikoussis NG, Apostolakis E, Papakonstantinou NA, Sarantitis I, Dougenis D. Safety of magnetic resonance imaging in patients with implanted cardiac prostheses and metallic cardiovascular electronic devices. Ann Thorac Surg. 2011; 91(6): 2006-2011.
17. Wollenweber SD, Ambwani S. Comparison of 4-class and continuous fat/water methods for whole-body, MRbased PET attenuation correction. IEEE Trans Nucl Sci. 2013; 60(5):3391–3398.
18. Soret M, Bacharach SL, Buvat I. Partial-volume effect in PET tumor imaging. J Nucl Med. 2007; 48:932–945.
19. Buether F, Jones J, Seifert R, Stegger L, Schleyer P, Schaefers M. Clinical evaluation of a data-driven respiratory gating algorithm for whole-body PET with continuous bed motion. J Nucl Med. 2020; 61(10):1520-1527.
20. Harteela M, Hirvi H, Makipaa A, Teuho J, Koivumaki T, Makela, MM et al. Comparison of end-expiratory respiratory gating methods for PET/CT. Acta Oncol. 2014; 53:1079–1085.
21. Dawood M, Büther F, Lang N, Schober O, Schäfers KP. Respiratory gating in positron emission tomography: a quantitative comparison of different gating schemes. Med. Phys. 2007; 34: 3067–3076.

22. Hope TA, Verdin EF, Bergsland EK, Ohliger MA, Corvera CU, Nakakura EK. Correcting for respiratory motion in liver PET/MRI: preliminary evaluation of the utility of bellows and navigated hepatobiliary phase imaging. EJNMMI Phys. 2015. DOI: 10.1186/s40658-015-0125-0.

Figures

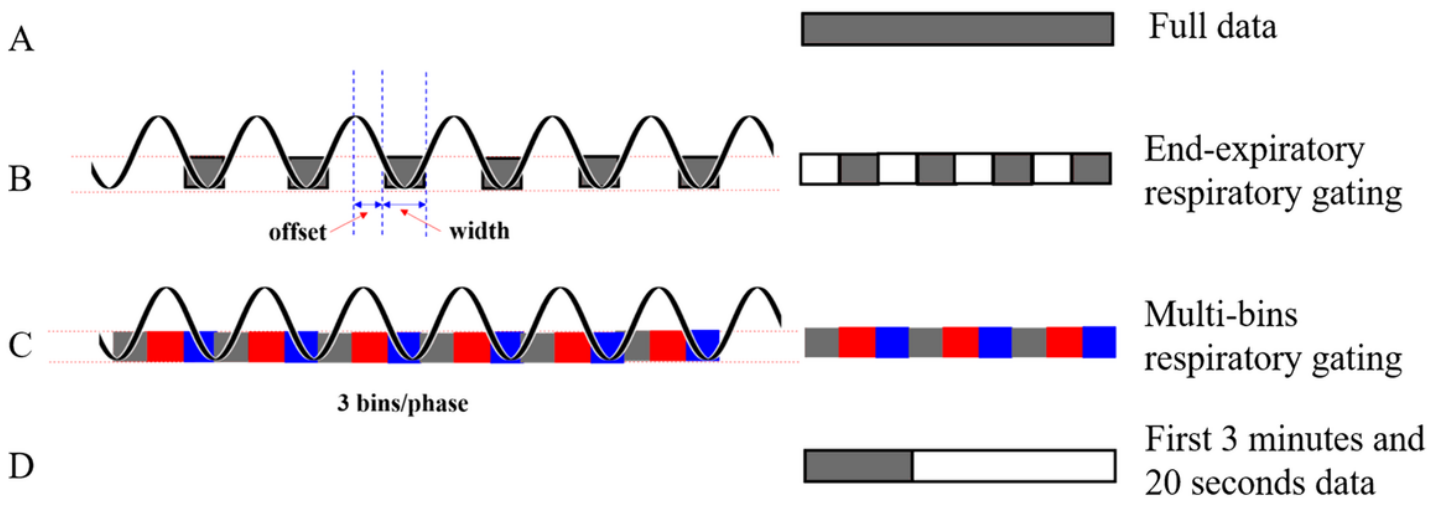

Figure 1

Four abdominal PET/MRI reconstruction methods. The left side of the figure shows the ideal respiratory cycle. The right shows diagrams of the four reconstruction methods

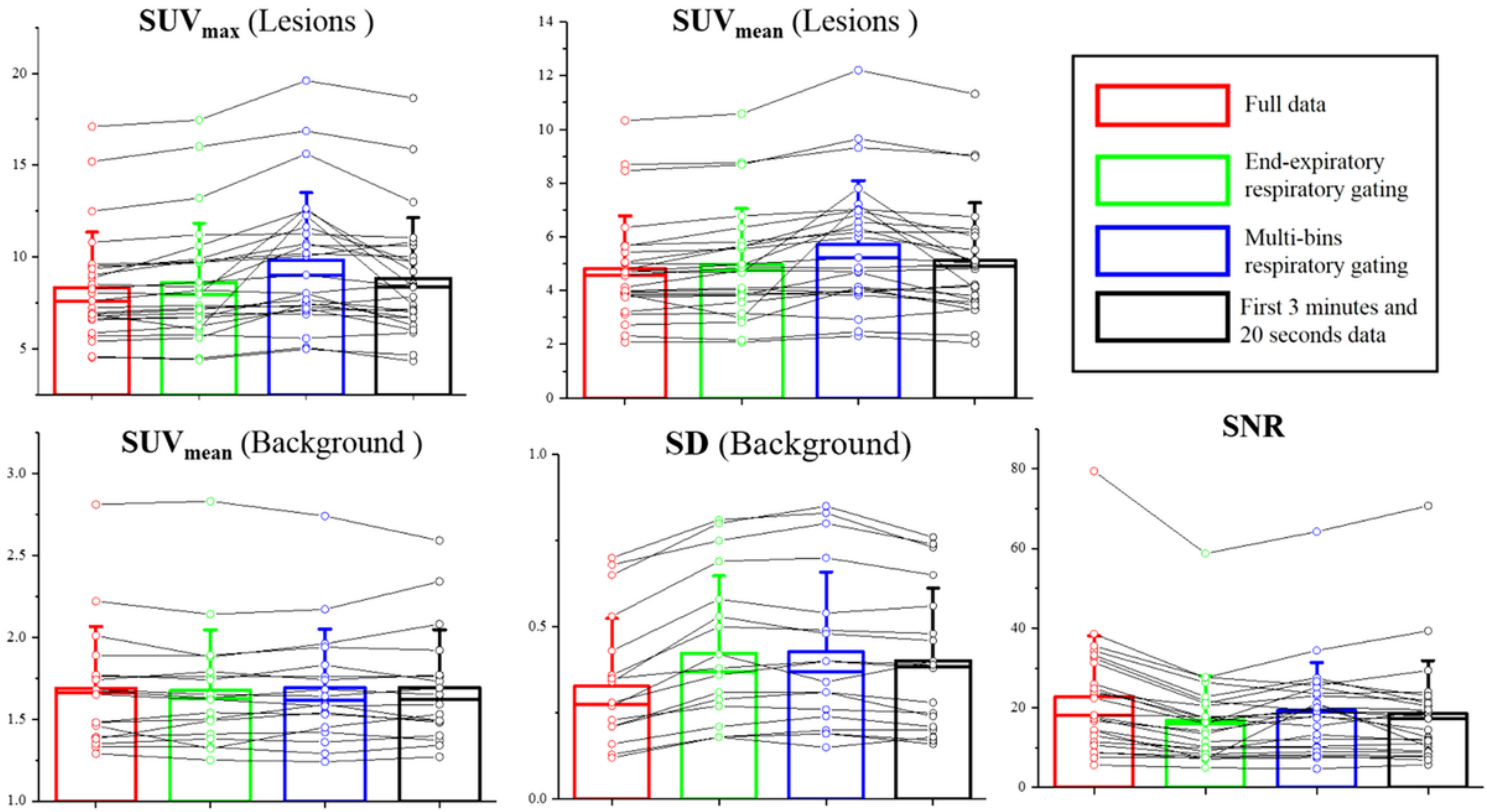

Figure 2

Means and standard deviations of the five parameters in the four groups. Different colours represent different groups, as shown in the top right corner. The detailed data are also shown by dots and the connected lines for visual paired comparisons.

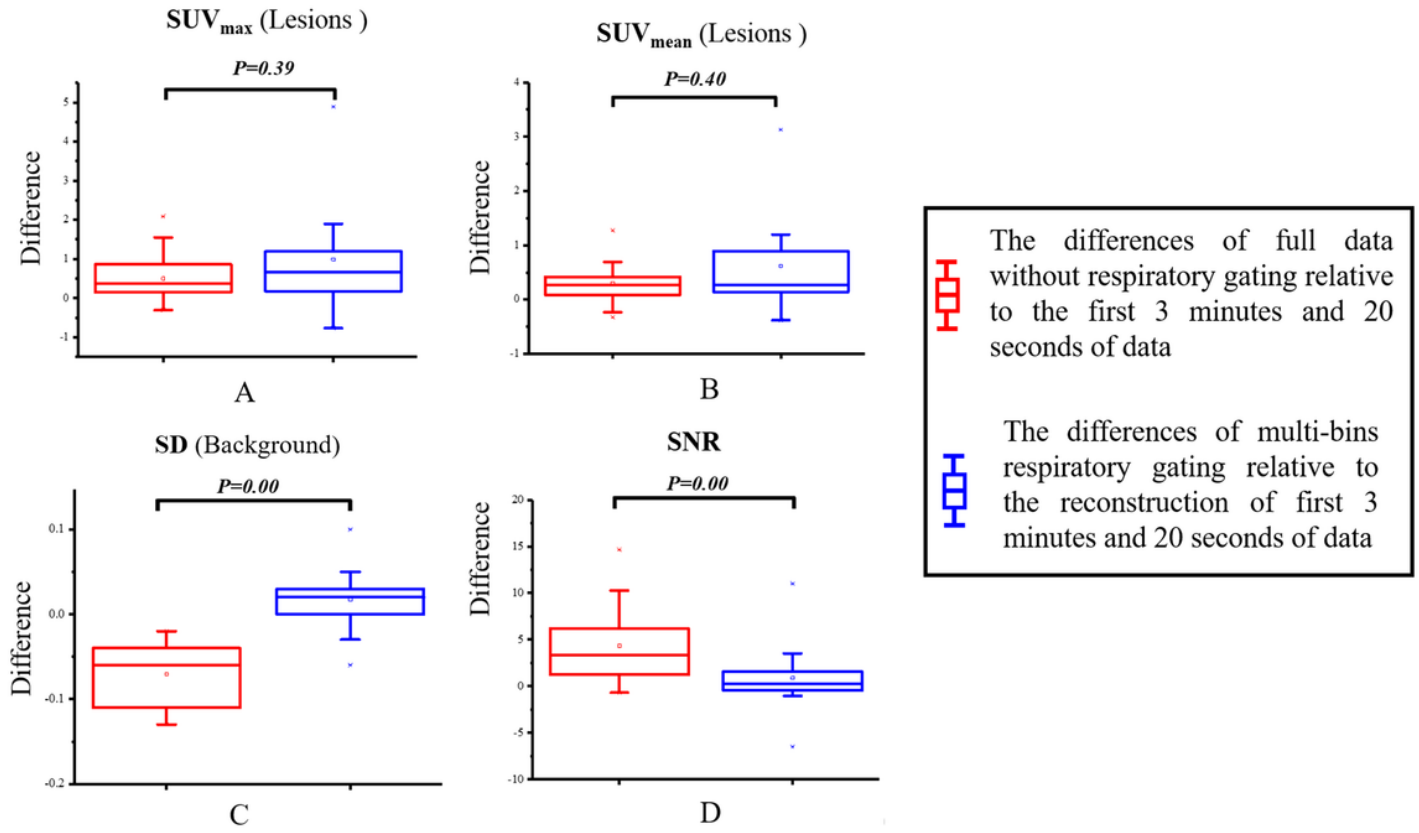

Figure 3

Comparison of difference among the reconstruction of full data without respiratory gating relative to the reconstruction of the first 3 minutes and 20 seconds of data (red boxes), the reconstruction of multi-bins respiratory gating relative to the reconstruction of first 3 minutes and 20 seconds of data (blue boxes), for four parameters, the SUVmax(A) and SUVmean(B) of lesions, the standard deviation of background(C) and SNR(D). The corresponding statistical results were also shown.

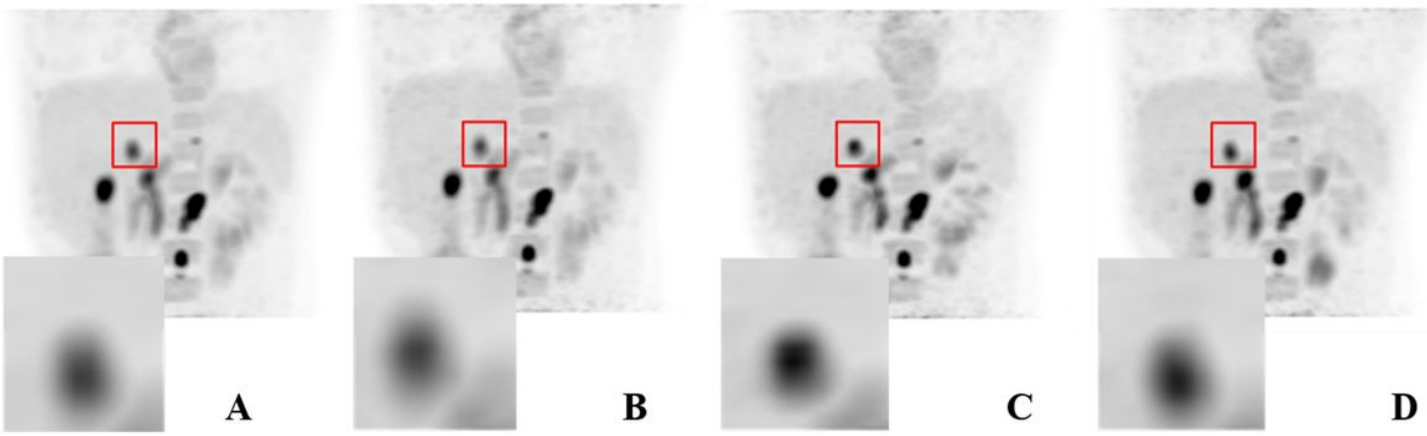

Figure 4

The representative patients' 3D MIP PET images reconstructed by the four methods, from left to right: reconstruction of full data without respiratory gating (A), end-expiratory respiratory gating (B), multi-bin respiratory gating (C), and reconstruction of the first 3 minutes and 20 seconds of data acquired without respiratory gating (D). The window centre and width were same for the four images.